Thermal Management Solutions for enhanced Digital Flight Data Acquisition Unit in Avionics Applications

Vicentiu Grosu, Chris Lindgren and Tamas Vejsz
Teledyne Controls
501 Continental Boulevard
El Segundo, CA 90245
Ph: 310-765-3769; Fax: 310-765-3115
Email: vicentiu.grosu@teledyne.com

Abstract
According to the Federal Aviation Administration, the commercial airline industry should expect to see the number of passengers traveling per year to grow from its current level of 750 million to nearly 1 billion by 2030. To meet this demand, airlines are placing orders for thousands of new aircraft over the next decade and beyond. With this increase in airline traffic, newer aircraft systems will generate an ever increasing amount of data per flight, data that allows airlines to further enhance their flight operations, flight safety, and reliability. For commercial avionics, the migration of the data acquisition and reporting functions from the traditional interface environments to newer, faster, and more network-centric architectures is creating a new generation of “smart” aircraft. Teledyne Controls’ enhanced Digital Flight Data Acquisition Unit is an integral part of a new generation of aircraft and combines the functions of Mandatory Data Acquisition and Recording with a sophisticated Aircraft Conditioning Monitoring System that the aircraft operator uses to monitor the performance and reliability of each aircraft in its fleet. Some of the critical goals in the development of the Digital Flight Data Acquisition Unit are reducing the size and weight over previous generations, while maximizing performance and reducing cost. All of these opposing requirements make the design and fabrication very challenging. One such challenge includes dissipating high power in a confined space, and this makes thermal management a critical component of the overall LRU (line-replaceable unit) design. In addition, to increase the reliability over the lifespan of the unit, passive cooling systems are often required in place of internal fans. This presents another set of challenges, such as optimizing the airflow provided by the aircraft in the electronics bay compartment. This paper will present some of the critical elements in thermal management such as heat sinks, components placement, thermal interface materials, thermal vias, thermal links, packaging approaches and cooling strategy. The design and optimization of the system are based on analytical solutions, conjugated heat transfer and experimental results. The LRU should safely operate under various environmental conditions: ground operation, flight operation, high operating temperature and loss of cooling air where each environmental condition has different parameters for coolant airflow rate, effect of the surroundings, and ambient and coolant air temperature. Draw-Through and Blow-Through cooling analysis were performed using CFD (Computational Fluid Dynamics). The thermal analysis problems solved are conjugated heat transfer for laminar flow with radiation in steady-state or transient regimes. Multiple approaches were identified to remove heat from the critical components through optimization of the components and subsystems. These same approaches can also be used to increase the system’s performance and reliability.

Key words
Avionics, CFD, electronics, packaging, thermal management

I. Introduction
Teledyne Controls’ enhanced Digital Flight Data Acquisition Unit (eDFDAU) (Fig. 1) is an integrated system that combines the functions of Mandatory Data Acquisition and Recording with a sophisticated Aircraft Condition Monitoring System (ACMS). This comprehensive system provides aircraft operators with a standardized hardware and software solution for high-power data acquisition, management and recording.

These functions require the inclusion of new processors and high speed interfaces such as Ethernet. The new equipment enhancements and add-ons challenge the limited space and power available in commercial aircraft and require that the new functionalities and features be packaged into small form factors in order to occupy the least amount of space in crowded aircraft electronics compartments. This requires designs that provide efficient thermal management while minimizing the weight, volume and cost. A similar trend is observed in the general electronics market, but the aircraft operation introduces additional constraints in term of high reliability in harsh environmental conditions making the design even more challenging.

Fig.1 eDFDAU – Enhanced Digital Flight Data Acquisition Unit

The thermal management solutions are strongly determined influenced by the demanding environment conditions which not only require creative design approaches, but could also constrain the system performance. Some of the harsh environmental conditions that need to be satisfied include temperature extremes (e.g. full performance between -40ºC and +70ºC ambient), high humidity, and vibration as dictated by existing standards addressing mechanical constraints and cooling requirements (ARINC 600 [1]). The environmental conditions limit the reduction in weight and cost of the avionics and are one of the main causes of reduced long-term reliability. Extreme temperatures were identified by US Air Force Avionics Integrity [2] as a factor in 55% of airborne electronic failures.

Even though the electronic packages of commercial aircraft are not subjected to the same, severe environment in terms of vibration, dust and humidity as the military avionics, efficient thermal control at elevated temperature is equally imperative to maintaining long-term reliability.

Decades of reliability data and analyses have shown that the reliability of integrated circuits is exponentially dependent on the temperature of the junction [3]. For instance, a 10-15°C reduction in junction temperature can serve to double the life expectancy of the device. An added benefit is the fact that the device performance often increases with the reduction of the junction temperature. Because of these factors, one of the most important targets of the design of thermal management of cooling system is maintaining the temperature of the cold junction below a set limit called the maximum junction temperature.

This paper will present several thermal design considerations for avionics electronics and describe some of the cooling methods used for thermal optimization in Controls' eDFDAU product. The goals of the thermal management solutions are to optimize thermal packaging, manage high heat flux levels, and maintain an optimum balance between weight, cost and performance. Challenges and opportunities for innovative solutions related to the avionics thermal management field will also be discussed.

II. eDFDAU Description

The eDFDAU is an ARINC 600 compliant avionics unit with dimensions of 12.6 in L x 7.5 in W x 7.6 in H. The chassis is made of aluminum sheet metal and houses several subassemblies as shown in Fig. 2.

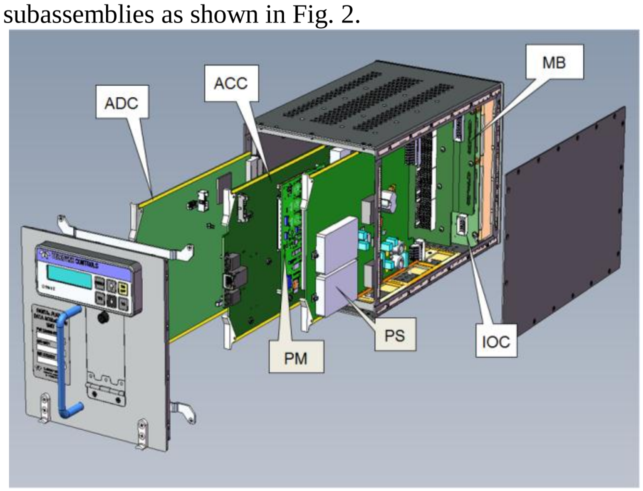

Fig. 2 eDFDAU

The subassemblies include:

- Analog-to-Digital Conversion Card (ADC)
- Acquisition Carrier Card (ACC)
- Processor Module (PM)
- Power Supply (PS)
- Input/Output Card (IOC)
- Motherboard Assembly (MB)

III. Cooling Elements

In our optimization and design we focus on the mechanisms that are significant to the thermal performance: convection (forced convection/natural convection) and the flow (approach air velocity / flow directions) that defines it and conduction, where the main driver is the heat sink thermal resistance. Also of interest is the integration in the cooling system where the heat sink pressure drop and the heat sink weight are important. The choice of heat sink material affects both the weight and the cost of cooling the unit. To achieve a robust thermal design for the eDFDAU, the following thermal elements are employed.

A. Air flow and its control features

The eDFDAU is a forced air cooled unit in accordance with ARINC 600. The unit can either receive forced-air cooling in a bottom to top direction (Blow-Through Cooling, BTC) or a top to bottom direction (Draw-Through Cooling, DTC). To ensure optimal heat removal, air flow control features within the chassis and the inlet position direct the cooling air to high heat dissipating areas. The location of the vents within the chassis is optimized by mounting the ADC and PS close to the side panels and positioning the PM1-ACC-PM2 assembly in the middle of the chassis. The mass flow rates used in the analyses are parameters in this optimization and are functions of environmental conditions and power dissipation. The analysis is conducted based on 40 Watts dissipation. Although there is some heat released from the exterior surfaces of the cooling unit by natural convection and radiation, the primary mode of heat transfer is by convective air cooling.

B. Heat Sinks

Heat sinks conduct the heat from the component level to regions where the air flow is stronger through elements (fins in the form of cylinders or ribs) that extend from the cooled surface. The additional heat transfer area of the fins correlated with the stronger flow around the fin surfaces results in a larger amount of energy being extracted from the cooled component. This, in turn, reduces the temperature of the cooled component for the same power dissipation. Auxiliary heat sinks have become integral parts of most thermal management systems as they are very versatile, reliable and relatively low cost. The PM module employs a finned aluminum heat sink (Fig. 3) that is linked to critical chips such as the main processor via thermal pads and metallic links.

Fig. 3 PM optimized aluminum heat sink

The fins, in the shape of rectangular plates, conduct the heat which is then transferred to the cooling air flowing along them through forced convection. The design ensures that the cooling path over the heat sink is not obstructed by any other objects in the assembly and that the flow is mainly along the fins as it reaches the heat sink to reduce the pressure drop. Heat sink optimization analysis was performed in order to determine the fin configuration that enhances the heat transfer between the PM module and the cooling air in the various design conditions (forced and natural convection). The parameter considered in this optimization was the fin pitch; the fin height was limited by the adjacent circuit card and was not varied. The fin was completely defined by selecting a fin thickness of 1.3 mm based on applicability to this problem and ease of manufacture.

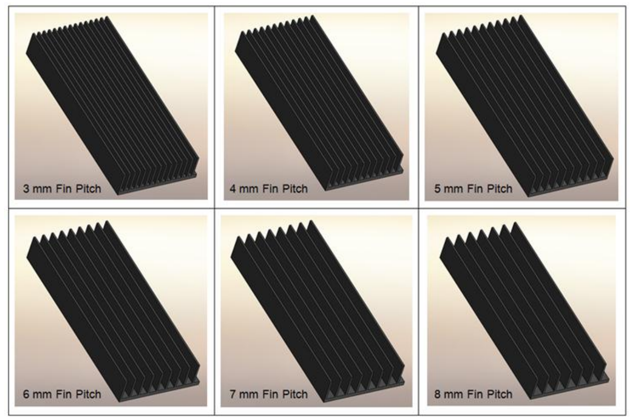

Fig. 4 shows the heat sink configurations considered in the analysis.

Table 1 Heat sink Comparison Forced Convection

Fin Pitch (mm)	ΔT forced (°C)	Pressure Drop (Pa)	Weight (g)
3	3.0	4.82	218
4	3.3	3.24	192
5	4.1	2.29	184
6	4.3	2.04	166
7	5.0	1.75	158
8	5.2	1.50	149

Smaller fin pitch leads to a lower temperature rise, as the heat sink cooling capability is increased by the increased cooling area. However, the smaller pitch results in a higher pressure drop. Fig. 5 shows the temperature rise per source.

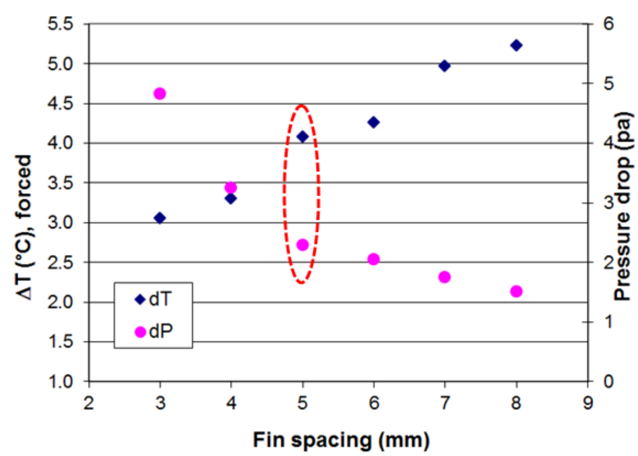

Fig. 5 Temperature Rise versus Heat Source (Forced Convection)

The heat sink with a 5 mm pitch is selected because it provides lowest component temperature rise and the smallest increase in weight and pressure drop.
The thermal analysis was further performed for the natural convection boundary condition.

Table 2 Heat sink comparison natural convection

Fin Pitch (mm)	ΔT natural (°C)	Weight (g)
3	30.7	218
4	26.5	192
5	23.5	184
6	22.0	166
7	20.6	158
8	19.8	149

Fig. 6 summarizes the temperature rise of the heat source for all six heat sinks considered.

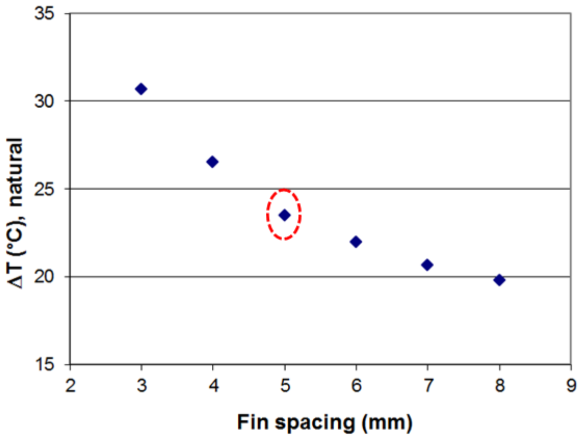

Fig. 6 Temperature Rise versus Heat Source (Natural Convection)

The primary cooling mechanism in this design is forced convection. We selected a heat sink with 5 mm fin pitch (our optimized heat sink) because it results in a mid-range temperature increase for natural convection with an acceptable pressure drop increase.
Radiation can be a major contributor in natural convection and low-airflow velocity applications. By black anodizing the surface of the heat sink (Fig. 3) the emissivity of the surface is increased. An additional benefit of the treatment is the increase in the corrosion, wear and electrical isolation.

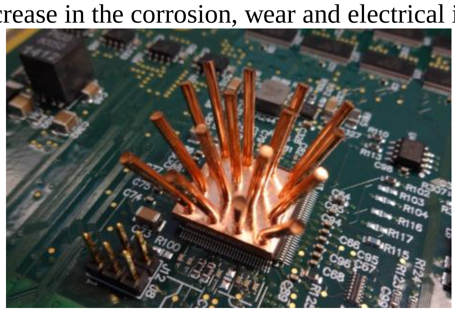

Fig. 7 Splayed Pin Fin copper heat sinks for Ethernet Switch

The Ethernet Switch also utilizes splayed copper pin-finned heat sink to cool the package Fig 7.
This part bonds directly to the top of the device package. Splayed pin fin heat sinks offer a highly efficient, omnidirectional cooling alternative for limited and moderate airspeed environments.

C. Thermal Interface Materials (TIM)

The conduction of heat from the component to the fins in the heat sink is strongly dependent of the thermal contact resistance at the interface between the heat sink and the component. Thermal interface materials reduce the thermal resistance by providing the pathway for the transfer of heat from components to heat sinks or PCB to heat spreader, etc. TIM significantly reduces the interfacial resistance between the top of the component surface (the heat source) and the bottom of the heat sink, allowing the heat to be conducted between these surfaces more effectively. Their selection is based on three parameters: the interface gap which the TIM must fill, the contact pressure and the electrical resistance of the TIM.This design employs TIM between the critical devices on the PM and the optimized PM heat sink and heatspreader (Fig. 8).

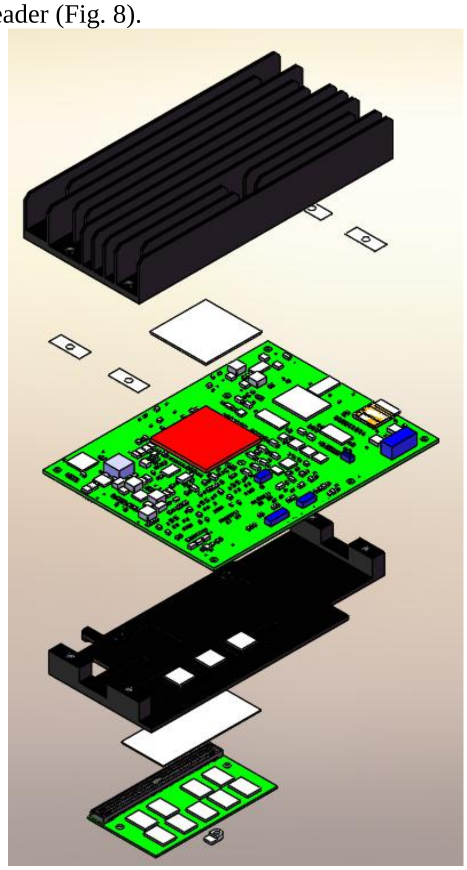

Fig. 8 PM heat sink and heatspreader with thermal interface materials

The TIM pads are used to thermally couple components of different heights to a heat sink or heat spreader. TIM pads are naturally tacky and don't require additional retention features other than being compressed between two surfaces. Another TIM consists of thermal tape which is used in the attachment of the pin fin heat sinks (Fig. 7). Thermal tape is the most cost effective of the heat sink attachments solutions, but it is suitable only for components with low power dissipation. The tape consists of thermally conductive carrier material with pressure sensitive adhesive on each side. The tape is applied first to the base of the heat sink and then the heat sink is attached to the component. The selection of the tape thickness has to optimize the adhesion (thicker tape is more "wetting") and the effect of decreasing the overall thermal resistance (thicker tape will have a larger thermal impedance).

D. Thermal Vias

Heat dissipation by conduction is also achieved through the board itself. Copper vias are (Fig. 9) dissipate heat from the copper surface layers, through the buried layers, to the back side of the PCB and then through the chassis wall where is removed by convection cooling. This effectively reduces the junction –to-ambient thermal resistance and contributes to maintaining acceptable junction temperatures.
The main benefit of enhanced vias is to reduce PCB heat resistance and to increase the spreading effect.

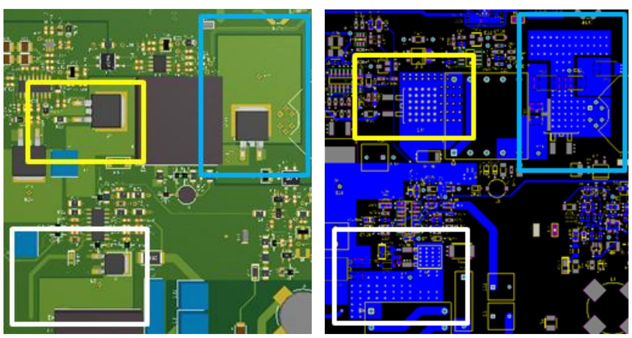

Fig. 9 CAD model and Gerber file for PS with vias

E. Heat Spreader

A heat spreader is generally used at critical locations where high power dissipation could result in hot spots. The strategic placement of heat spreaders even out the temperature eliminating hot spots and remove the heat in a more efficient fashion. These increase the lifetime of the power dissipating components and improves their performance. In our study, an aluminum heat spreader is applied to the back of the PM and dissipates the heat from Ethernet Phy (Fig. 8).
Aluminum has a lower thermal conductivity than copper, but it is still high enough that, in conjunction with its low cost, low density and superior manufacturability makes it a very attractive option for heat spreader fabrication.

IV. Boundary Conditions and Thermal Analysis

The simulations of this conjugated heat transfer problem including radiation were conducted using ANSYS Icepak V15, under different flight conditions and cooling modes. Because the unit is located in an open environment, the computational domain was extended beyond the enclosure to capture the natural convection effect consisting of the thermal plume. The equations involved in the heat transfer are: continuity equation, Navier-Stokes equations and energy equation for incompressible laminar flow. Natural convection was included in the simulations by employing the Boussinesq approximation that accounts for the buoyancy effect. The radiation heat transfer was simulated with Ray tracing model. Ambient pressure and ambient temperature were specified on the domain boundaries.
The computational domain was divided into discrete control volumes. Because the system has a very complex geometry we applied non-conformal mesh for local refinement to control the mesh density and improve the mesh quality around specific components while keeping the overall mesh size manageable. The grid resolution and grid quality were ensured for solution accuracy and computational stability. A grid-independent study was also carried out. The chosen mesh has the size of 6.8 million control volumes.
Because of the complicated geometry and the heat transfer modes the double-precision solver was used to reduce the round-off errors for this problem. Body-force weighted discretization scheme was chosen for pressure, and first-order discretization scheme was for momentum and energy equations. In addition to the convergence criteria for flow and energy equations, we also set monitoring points for temperature, velocity and pressure. The convergence was determined by monitoring solution residuals while making sure that values at the monitoring points did not change anymore. The converged solution was obtained after 1000 iterations.

V. Results and Discussion

All the circuit card components were reviewed for expected power dissipation during operation. If an active part was found to dissipate more than 0.5 Watt, that part was independently modeled into the analysis and their power was directly applied to the proper package size and board location. The PCBs are modeled as solid homogeneous materials, but their thermal properties used in the simulation accounted for the number of copper and insulator material layers, their thicknesses, and the percentage of copper in each layer. The PCB vias were implemented without simplification in the model. Network blocks are used to model a component when junction-to-case and junction-to-board thermal resistances are available from supplier; otherwise, the components are modeled as solid blocks with volumetric heat dissipation. When thermal interface materials (solder joint or thermal pad) are used, the simulation captures them through thermal resistance. Simulations are performed to demonstrate the eDFDAU unit maintains reliable and safe temperature under the design environments tabulated in table 3.

Table 3 Design Environments

DESIGN ENVIRONMENT	Coolant Airflow Rate (kg/hr-kw)	Blow-Through Cooling		Draw-Through Cooling	Effect of surrounding units
		Ambient (°C)	Coolant Air (°C)	Ambient/Coolant Air (°C)	
Normal Ground Operation (NGO, steady-state)	220	50	40	50	Radiation from 60°C surface
Normal Flight Operation (NFO, steady-state)	136	50	30	50	Radiation from 60°C surface
Short-Time Operating High Temperature (STOH, 30 minutes)	220	70	70	70	NA
Loss of Cooling (LOC, 90+ minutes)	NA	40	NA	40	Radiation from 60°C surface

A. Air Flow and Temperature Distribution

Air enters through the top inlet at 11 kg/hr mass flow rate (roughly 1 m/s inlet velocity) and then passes through an internal baffle plate. The baffle plate ensures that the air is directed primarily over the PM1 and PM2 heat sinks and the key components for PS, ACC and ADC printed circuit boards. The maximum pressure drop obtained for this enclosure design is approximately 1.01 inch H_20 making it compliant with the chassis pressure drop requirement of 1 ± 0.1 inch H_20 per ARINC 600.

The pressure drop indicates that the packaging design maintains the expected resistance in the aircraft rack. The flow resistance introduced by the baffle creates a region of pressurized air between the top of the chassis and baffle which produces "jets" of high velocity that exits the holes in the baffle as shown by the fingerlike isothermal profiles in Fig. 10. Several configurations were simulated for the cooling holes placement and size to establish the optimal pattern. The holes are distributed in the baffle to direct the air over the high heat dissipation components: the first row of holes drives the air over the PS components; the second and the sixth row of holes direct the air through the PM1 and PM2 heat sinks; the remaining holes guide the air flow towards the Ethernet Switch heatsink and memory modules. High velocity air over the heat generating components increases the heat transfer coefficient and improves the mechanism of heat removal.

The velocity vectors and temperature contours of the cross-section through the center of 1^{st} row of holes can be seen in Fig. 10. The plot clearly shows high velocity flow at the location of the holes at both inlet and outlet; a higher velocity is also observed in regions farther away from the holes – still in the main path between inlet and outlet. The regions away from the flow path exhibit a low velocity. As expected, the plot of the isotherms shows distinct lower temperatures in the areas with the high velocity flow of cooler air. High velocity continues to travel farther in the enclosure ensuring proper cooling for key power supply components.

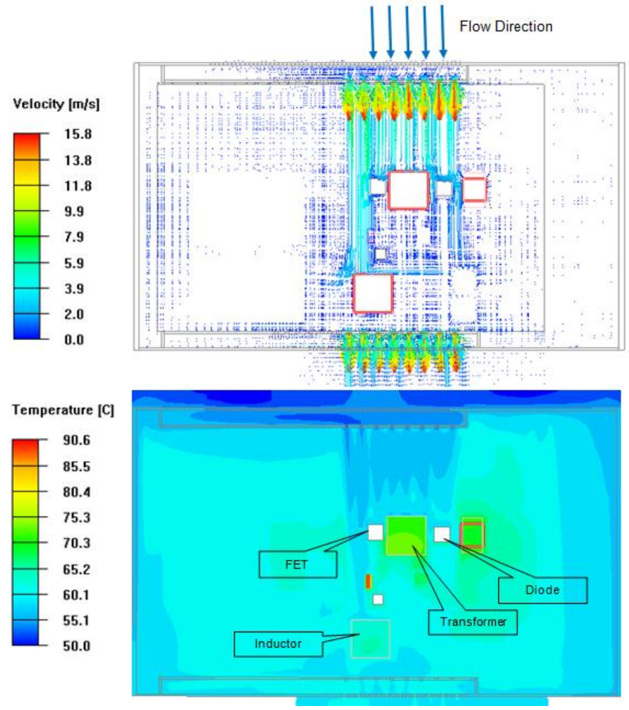

Fig. 10. Velocity vectors and temperature contours of the cross-section through the center of 1^{st} row of baffle openings over PS

Fig. 11 corresponds to the cross-section thru the center of 2^{nd} row of holes and shows the velocity vectors and temperature contours. In this cross-section, it is clear that the main power dissipation is from the PM1 heatsink. The aligned flow (PM1 heatsink fins and the inlet holes) causes the air at the inlet holes to flow evenly between heatsink fins, producing the desired cooling effect in the PM heatsink.

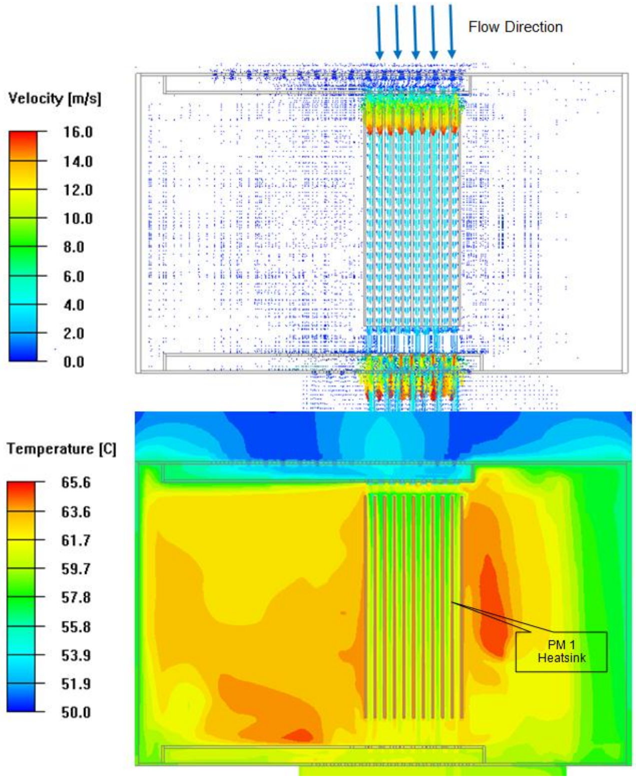

Fig. 11. Velocity vectors and temperature contours of the cross-section through the center of 2[st] row of baffle openings over PM1 heatsink

The velocity vectors and temperature contours of the cross-section thru the center of 3[rd] row of holes can be seen in Fig. 12. The effect of high velocity flow at the exit from the baffle holes is also present in this cross-section. The plot shows that the high velocity air is directed towards the memory module from PM1 module in order to assure proper cooling of the memory module chips.

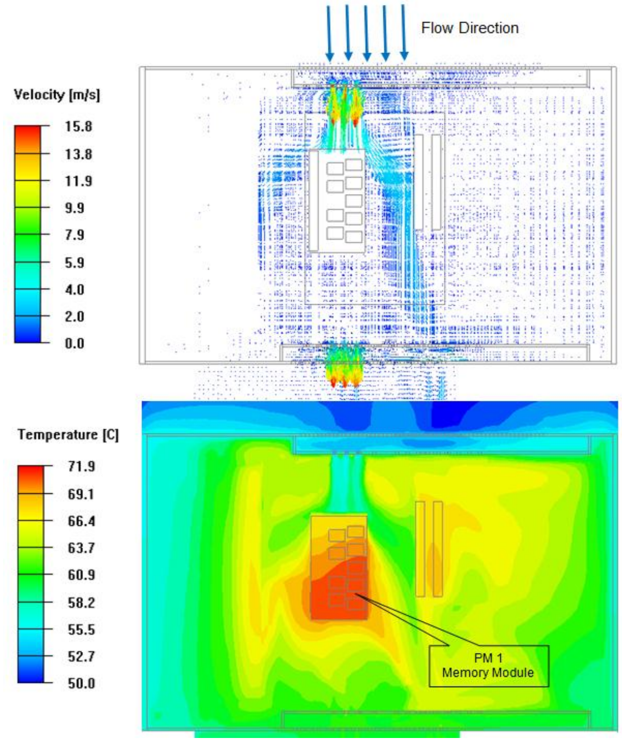

Fig. 12. Velocity vectors and temperature contours of the cross-section through the center of 3[rd] row of baffle openings over PM1 memory module

Similar results were observed for PM2 heatsink, PM2 memory module and Ethernet Switch.

B. Chassis Touch Temperature

The chassis surface temperature is required to remain below 15˚C above ambient temperature. Fig. 13 shows the temperature contours for the chassis outer surface. The ambient is considered 50°C during Normal Ground Operating Temperature. The chassis maximum temperature is 61°C, 4°C below the limit temperature.

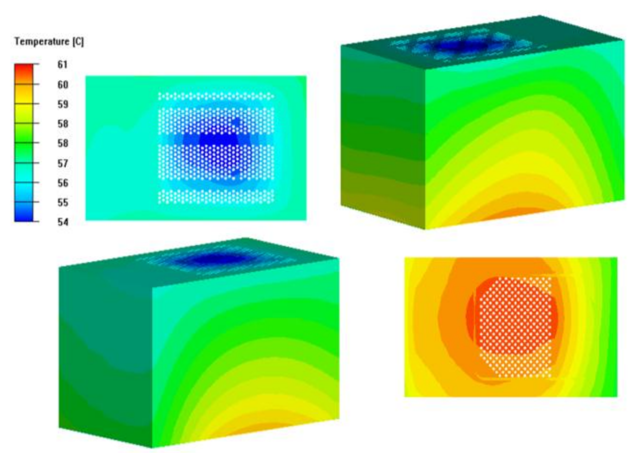

Fig. 13 Chassis Surface Temperature

C. Component Temperature

Normal Ground, Normal Flight and High Operating conditions are simulated under steady state regime. Fig. 14-16 present the Blow-Through Cooling and Fig. 17-19 show the component surface temperature for Draw-Through cooling. The temperature scale for the subsequent Fig. 14-19 is fixed to 40°C – 125°C to allow the comparison between various design environments.

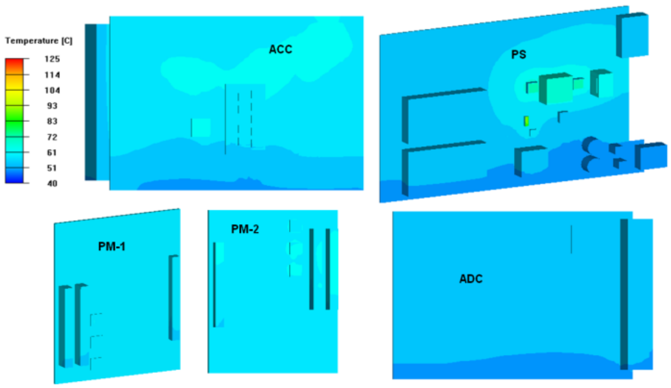

Fig. 14 NGO Blow-Through Cooling – component temperature contours

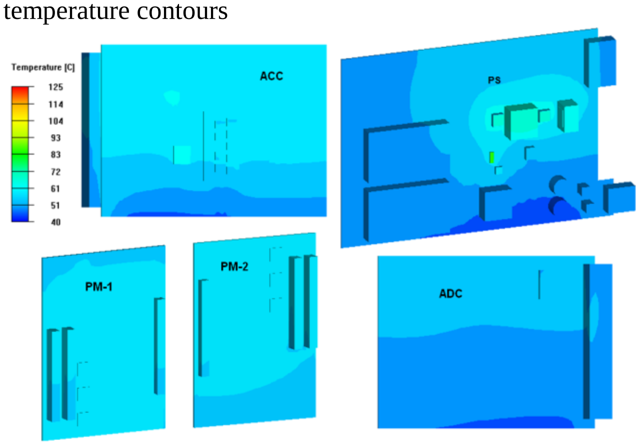

Fig. 15 NFO Blow-Through Cooling - component temperature contours

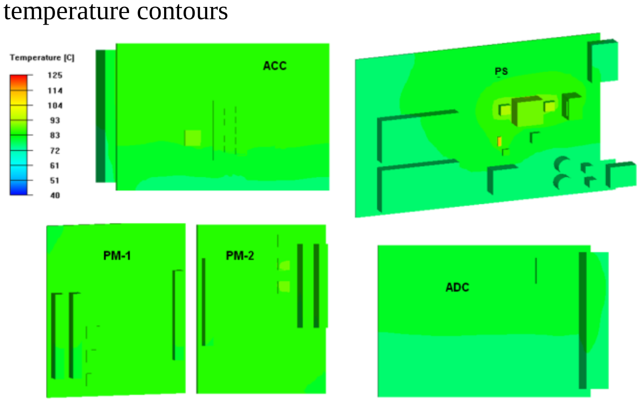

Fig. 16 STOH Blow-Through Cooling - component temperature contours

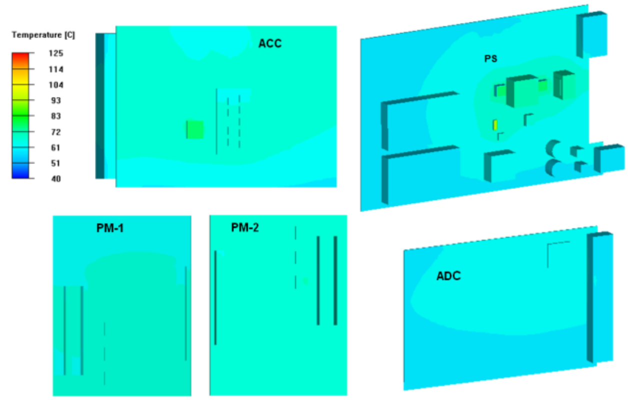

Fig. 17 NGO Draw-Through Cooling - component temperature contours

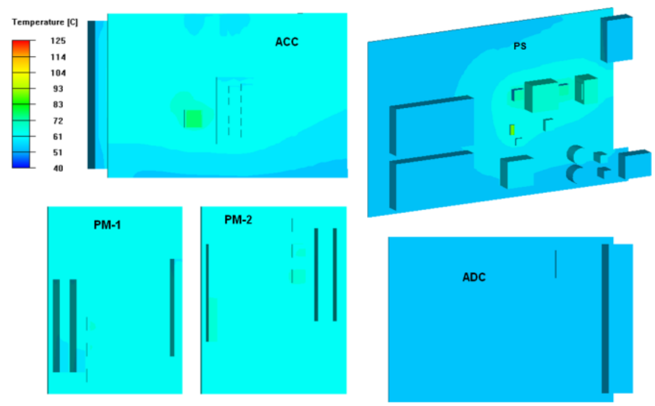

Fig. 18 NFO Draw-Through Cooling – component temperature contours

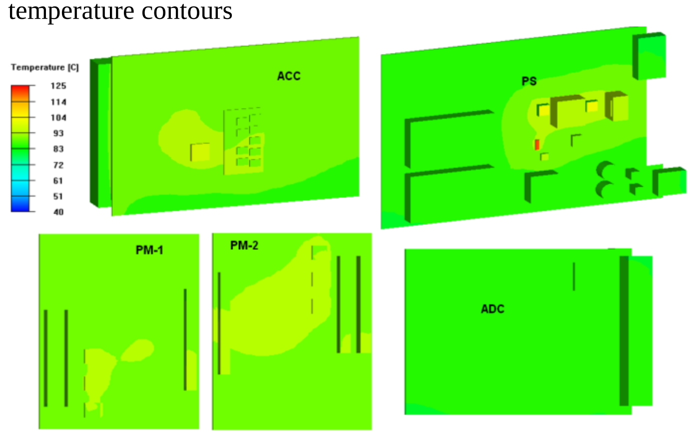

Fig. 19 STOH Draw-Through Cooling - component temperature contours

When comparing the steady stage analyses for the various operating conditions, the highest (between the various simulated conditions) of the maximum (between components) component temperature occurs during the STOH-Draw Through Mode. This is a result of the higher temperature of the cooling air and the fact that the Draw Through Mode causes smaller velocities compared to the Blow Through mode.

D. *Maximum Component Temperature*

The most stringent condition is represented by the Loss of Cooling (LOC). It assumes that there is no air flow and the only losses are through radiation and natural convection. The safety requirements are specified in terms of temperatures at 90 minutes after the loss of cooling. Due to the time dependency, the thermal analysis was performed as a transient analysis initialized from a steady state analysis at normal flight operation (NFO). At the start of the transient analysis corresponding to the loss in cooling, the inlet air flow was set to zero. Fig. 20 presents the junction or the maximum component temperature as a function of time for each component of PS.

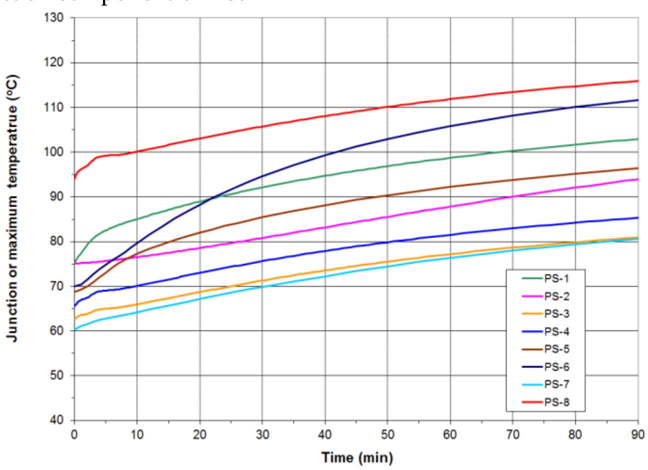

Fig. 20 LOC – Junction or maximum temperature vs time for the components located on PS.

The results indicate that the junction temperature are all below the maximum temperatures specified by the component manufacturers.

VI. Conclusion

This paper presents several approaches for enhancing the heat removal from the eDFDAU components. ANSYS Icepak V15 was used to simulate the approaches considered under the constraint introduced by the available air flow and under various operational and environmental conditions. The design configurations employed all means for improving the overall heat transfer from the components to the environment. These included optimization of the heat sink geometry, reduction of the thermal resistance at the interfaces between the components, and distribution of the flow in the enclosure to enhance the cooling around the high power dissipation components. The heat sinks were optimized as stand-alone elements. The reduction in thermal contact resistance was achieved by selecting the best suited materials. The entire eDFDAU unit with the selected heat sinks and TIM was modeled to evaluate the influence of the air flow distribution on the temperatures of interest (component and junction temperature, touch temperature) under several design environments.

The simulations of the selected enclosure configuration showed that, by using baffles with strategically placed holes, the flow can be redirected to the power dissipating components. The cooling effect of the flow was such that the thermal requirements were satisfied. Moreover, the additional hydraulic resistance introduced by the flow control features did not increase the overall pressure drop beyond the acceptable value.

The simulations also confirmed that the temperature of the components remained under the manufacturers' maximum values for all design environments and operating conditions. The chassis touch temperature was only 11ºC above the environment temperature, lower than the required 15ºC. Even under the more stringent STOH and LOC conditions, the temperature of the electronic components and the maximum junction temperatures had acceptable values. The temperatures were also below the de-rated maximum junction temperature for (NGO and NFO) conditions using Blow / Draw Through Cooling.

In conclusion, the challenge introduced to the airborne electronics by the size, weight and power requirements can be met by detailed thermal analysis and the thorough understanding of the critical components in the cooling mechanism. By combining stand-alone selection (TIM) and simulation (heat sink) with entire system simulations that account for forced and natural convection, conduction and radiation, a design configuration that meets the requirements of modern commercial aircraft application can be established and validated.

References

[1] "ARINC Specification 600-19: Air Transport Avionics Equipment Interface", *Aeronautical Radio, Inc.*, 2011.

[2] M. Reynell, "Thermal Analysis Using Computational Fluid Dynamics," *Electronic Packaging and Production* 30, no. 10, 1990, pp. 82-88.

[3] R.Viswanath, V. Wakharkar, A. Watwe, and V. Lebonheur, "Thermal Performance Challenges from Silicon to Systems," *Intel Technology Journal*, Q3, 2000, pp. 1-16.